

A new control strategy for tracking peak power in a wind or wave energy system

S. Srinivasa Rao*, B.K. Murthy

Department of Electrical Engineering, National Institute of Technology, Warangal 506 004, Andhra Pradesh, India

ARTICLE INFO

Article history:

Received 15 July 2008

Accepted 9 November 2008

Available online 27 December 2008

Keywords:

Wind energy

Wave energy

Induction generator

Peak power tracking

ABSTRACT

This paper proposes a novel control strategy for tracking peak power in a wind or wave energy system using a squirrel cage induction generator. It eliminates wind speed measurement or estimation and uses a simple scalar technique by exploiting the cubic nature of the power curve. The method works even when air velocity is varying dynamically.

© 2008 Elsevier Ltd. All rights reserved.

1. Introduction

Today, more than 80% of the world's electric power generation comes from fossil-fuelled plants. With conventional energy sources becoming scarce and the demand for energy on the increase, alternative and inexhaustible sources of energy have to take their place. Since the input to these systems is free, energy efficiency is often overlooked. As a result, the installation costs become higher and the systems become oversized and are unable to compete economically with conventional systems. Hence there is a need to operate non-conventional energy systems optimally so that they extract maximum power from the available input source.

1.1. Review of peak power extraction strategies

The power developed by a wind or wave turbine depends not only on the air velocity but also on the speed of the turbine. The speed at which maximum power is developed is a function of air velocity. In order to extract maximum power, the speed of the turbine has to be controlled as a function of air velocity. Various researchers have proposed different control schemes. Some controller designs employ anemometers to measure wind velocity [1]. These mechanical sensors increase the cost and reduce the reliability of the overall system. The measurements can be seriously perturbed by turbulence. Due to the difficulties in wind

speed measurement, a control strategy based on the tip-speed ratio is practically difficult to implement. Consequently methods of wind speed estimation have been suggested [2,3]. A simple perturb and check algorithm is a straightforward solution to the maximum-power-point tracking problem. However, this method has the drawback of being 'fooled' if the turbine torque-speed characteristic is changing as a result of wind fluctuations while tracking is being done. Wind speed estimation is difficult in highly variable wind speed conditions. Hence control strategies have been proposed by some researchers that do not require wind speed information. These controllers use direct power measurement and elaborate search techniques to track the maximum-power-point. Quite often sophisticated field oriented control techniques are used to determine the power flow in the motor [4–6]. With field oriented, control advanced current regulated converters and methods of measuring flux or rotor position are required. Such requirements add to the cost and complexity of the converter. Fuzzy logic control techniques and neural network techniques [7–11] provide robust control of maximum wind power extraction. With such sophisticated techniques the cost and complexity of the system increase. Some control schemes require online search strategies for maximization of power. This requires wind speed to be relatively constant during the search operation. However, such strategies fail when wind speed is highly variable.

2. The proposed scheme

The approximate equivalent circuit of a three-phase squirrel cage induction generator is shown in Fig. 1.

* Corresponding author. D-2/2, NIT Staff Quarters, Warangal 506 004, Andhra Pradesh, India. Tel.: +91 9440413982.

E-mail address: srinivasarao_nitw@yahoo.co.in (S.S. Rao).

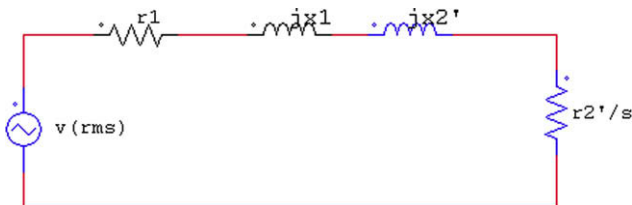


Fig. 1. Per phase steady state approximate equivalent circuit.

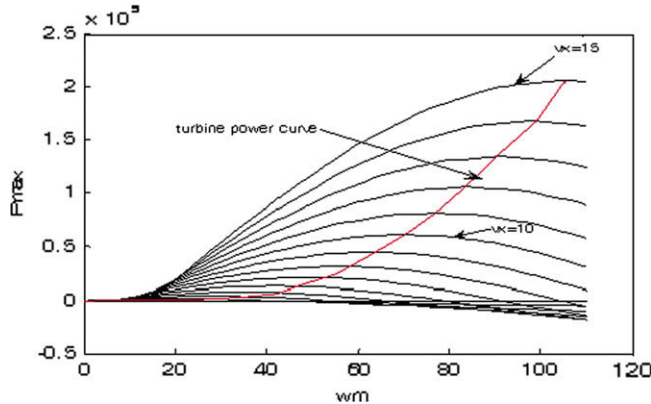


Fig. 2. Speed-power characteristics for a wind turbine.

The air gap power is given by

$$P_g \equiv 3V^2 s / r'_2 \propto V^2 s$$

To extract maximum power, slip loss must be kept small. This is achieved by operating the generator at a low slip by variable frequency control. However, it is not possible to reduce the frequency alone, as it will result in magnetic saturation of the core. In steady state, if the applied voltage were kept directly proportional to the frequency, the current in the machine would remain essentially constant at most frequencies and saturation would be avoided. This is the essence of V/f control [12]. The drawback with V/f control is that whereas torque follows a square law, the flux

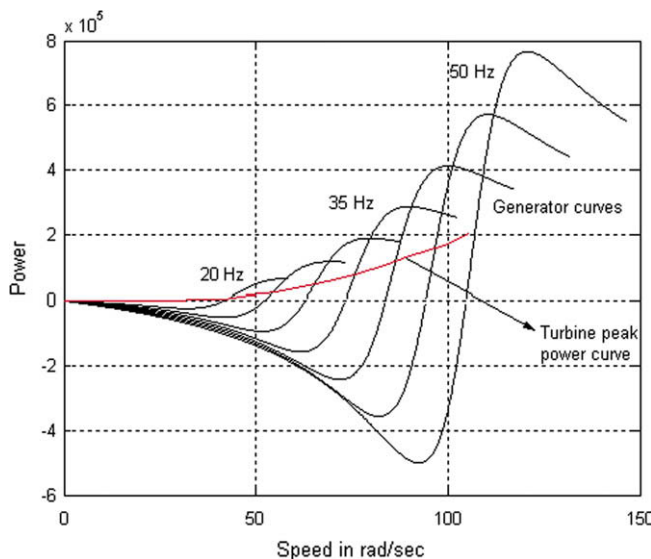


Fig. 3. Generator curves for V/f^2 control superimposed on turbine peak power curve.

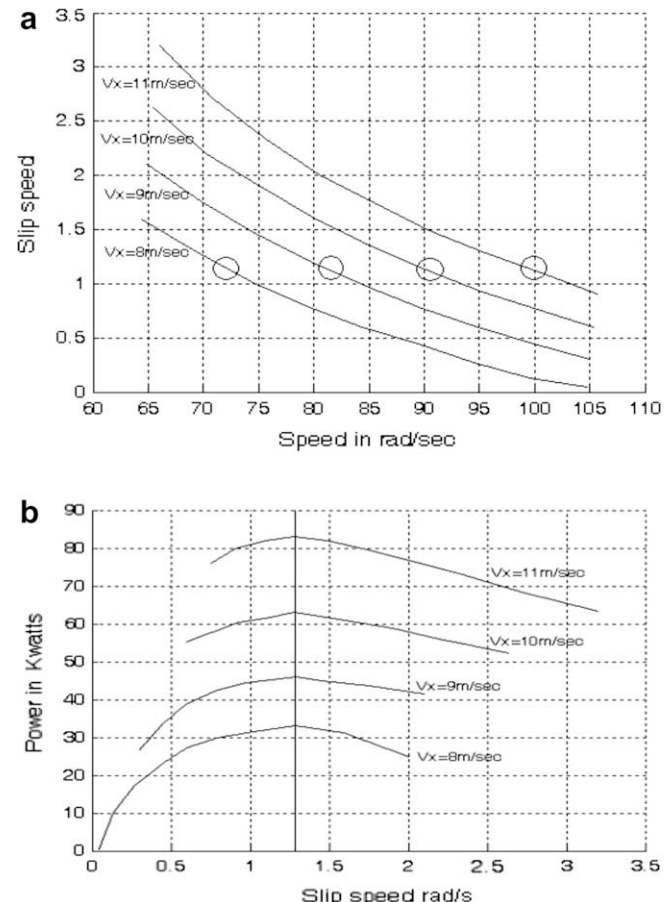


Fig. 4. (a) Slip speed vs. rotor speed in V/f^2 control for various air velocities. (b) Stator power vs. slip speed in V/f^2 control for various air velocities.

remains constant, resulting in high core losses and reduced efficiency. As suggested by Nola [13], it is unnecessary to provide rated flux when the generated torque is low. At lower torque levels, excitation can be reduced. Since core losses are directly related to flux level, reduced flux helps to reduce core losses thereby increasing the generated power. This saving is not possible under V/f control.

The above drawback can be removed by weakening the flux at lower speeds, i.e.

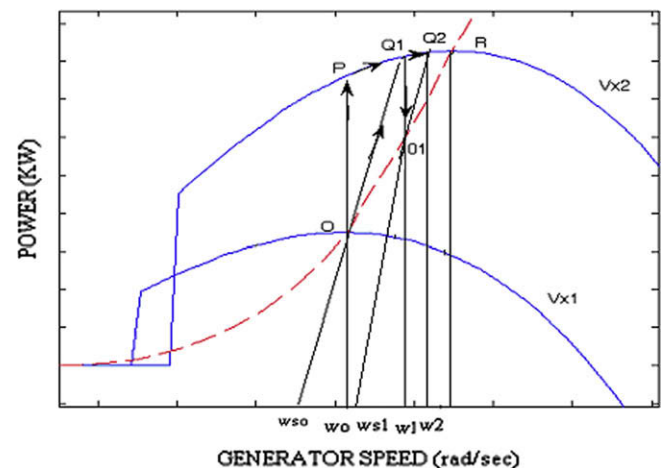


Fig. 5. Shift of operating point in the proposed strategy.

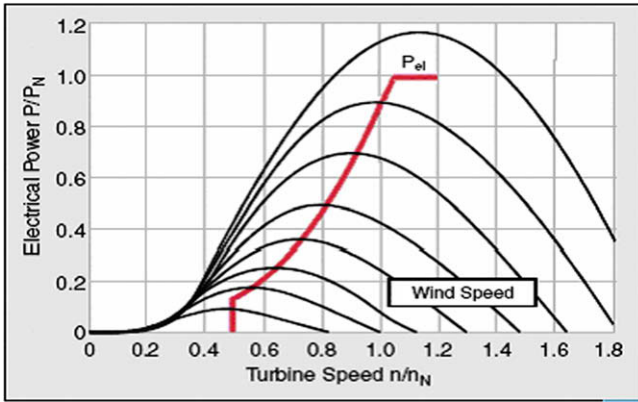


Fig. 6. Operating limits to be observed by the controller (when power limit is reached earlier than speed limit).

$$V/f \propto f$$

or

$$V \propto f^2$$

When the peak power points of a wind or wave turbine are joined, they are found to lie on a cubic curve as shown in Fig. 2.

$$P_g \propto \omega_m^3$$

But $\omega_m \propto f$ since slip is negligible.

$$\text{Hence } P_g \propto f^3.$$

Since $P_g \propto V^2 s$ as derived earlier, we get

$$f^3 \propto V^2 s = f^4 s$$

Therefore $s f = \text{constant}$.

Hence to be able to track peak power in this scheme, the slip speed at the peak power points must be maintained constant.

Fig. 3 shows the power-speed curves of a typical wind turbine for various air velocities with induction generator curves for constant $V/f^2 = V_{\text{rated}}/f_{\text{rated}}^2$ superimposed on them.

The points of intersection of the various turbine and generator curves can be translated into slip speed vs. rotor speed as shown in Fig. 4a. The sign of the slip speed (negative) has been ignored. Similarly a plot of stator power vs. slip speed is shown in Fig. 4b.

We observe that maintaining slip speed constant results in maximum power extraction. The controller measures the shaft speed, adds the fixed slip speed value (negative) to determine the synchronous speed and hence stator frequency required.

The supply voltage is determined from the relation

$$V = K f^2 \text{ where } K = V_{\text{rated}}/f_{\text{rated}}^2$$

The flux level is proportional to V/f . Since $V/f \propto f$, the flux level reduces in proportion to frequency and hence with generated torque and power. This removes the main drawback of V/f control, namely constant excitation at all loads, resulting in higher core losses. In the proposed scheme, losses are greatly reduced at light load, thus increasing the generated power.

3. Proposed control strategy

The strategy is explained with reference to Fig. 5, in which the curves of a wave turbine for two different axial air velocities are superimposed on the steady state induction generator curves for constant V/f^2 . Assume that the turbine is operating at point O corresponding to air velocity Vx_1 . The corresponding rotor speed is ω_0 and the synchronous speed of the generator is ω_{s0} , which has been determined by the controller to maintain the programmed value of slip speed ($\omega_0 - \omega_{s0}$). This ensures that O is the peak point for Vx_1 . The generator power speed curve for this condition is OQ1. The system is in equilibrium since both turbine power and

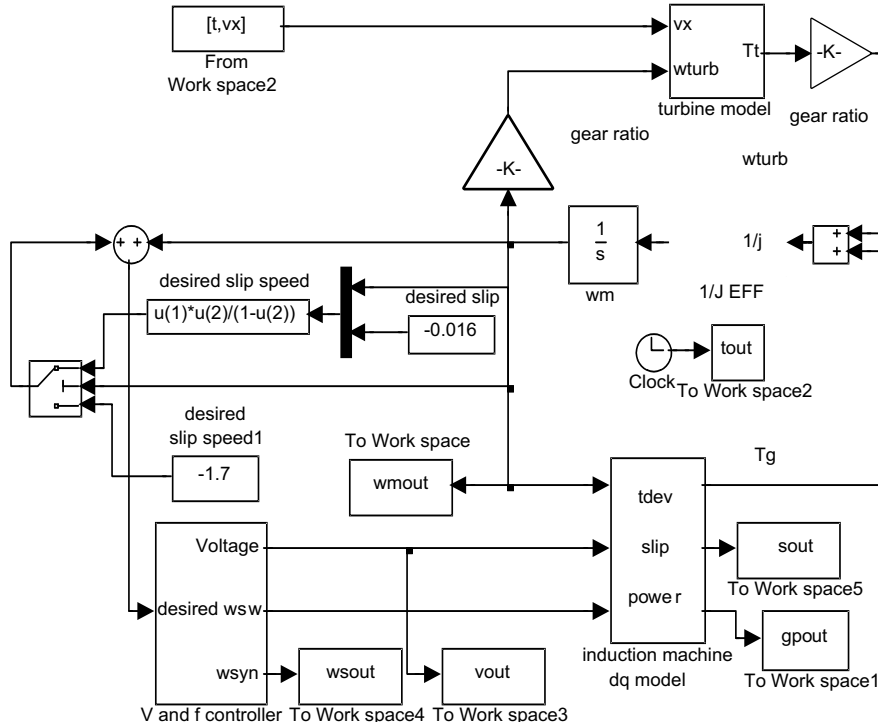


Fig. 7. SIMULINK diagram for the complete wave energy system.

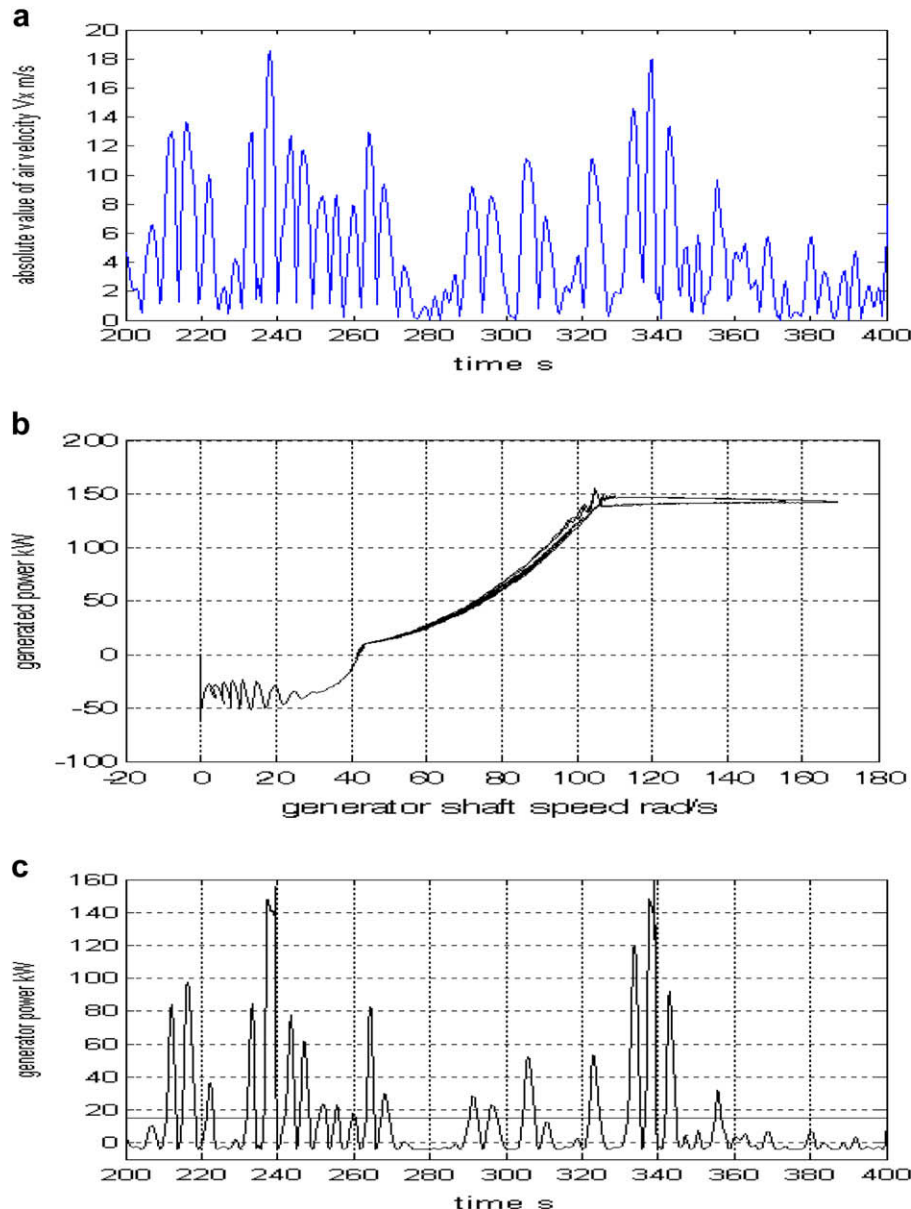


Fig. 8. (a) Rectified waveform of air velocity collected from the wave energy site. (b) Simulated power vs. speed showing controller modes. (c) Time variation of generated power for the actual air velocity taken from the wave energy site.

generator power are the same. Hence there is no acceleration or deceleration.

Suppose air velocity changes from Vx_1 to Vx_2 . There are two extreme cases to be considered: if inertia is high, or if air velocity has changed instantaneously, then rotor speed remains at ω_0 during this transition and the turbine power jumps to point P, whereas generator power remains at point O. Since turbine power is greater than generator power, the system accelerates. Therefore speed rises above ω_0 , turbine power moves from P towards Q1 along the turbine curve, generator power moves from O towards Q1 along the generator curve (assuming that the generator voltage and frequency have remained unchanged, i.e. the controller is inactive).

If inertia is negligible, or if air velocity changes very slowly, then both the turbine and generator will move along the generator curve OQ1 via turbine curves corresponding to intermediate air velocities. Turbine power is almost equal to generator power throughout the transition since there is negligible inertia power. (Again it is

assumed that the generator voltage and frequency have remained unchanged, i.e. the controller is inactive.)

In a practical system, the turbine moves along some path from O to Q1 which is between the above two extreme paths, namely OPQ1 and OQ1. Finally the operating point for both generator and turbine will be Q1, at which the rotor speed is ω_1 and slip speed has increased from $\omega_0 - \omega_{s0}$ to $\omega_1 - \omega_{s0}$ (assuming that the controller has not acted).

Now consider the action of the controller. According to the proposed strategy, slip speed must be maintained constant. Hence the controller increases the synchronous speed to ω_{s1} such that $\omega_1 - \omega_{s1} = \omega_0 - \omega_{s0}$. The new generator curve is O1Q2. Hence the generator operating point jumps down from Q1 to O1 whereas the turbine operating point remains at Q1. The turbine power is again greater than generator power. This difference accelerates the system further to speed ω_2 , where the turbine power and generator power become equal.

But the slip speed has again increased. So the controller increases the synchronous speed further. This process continues

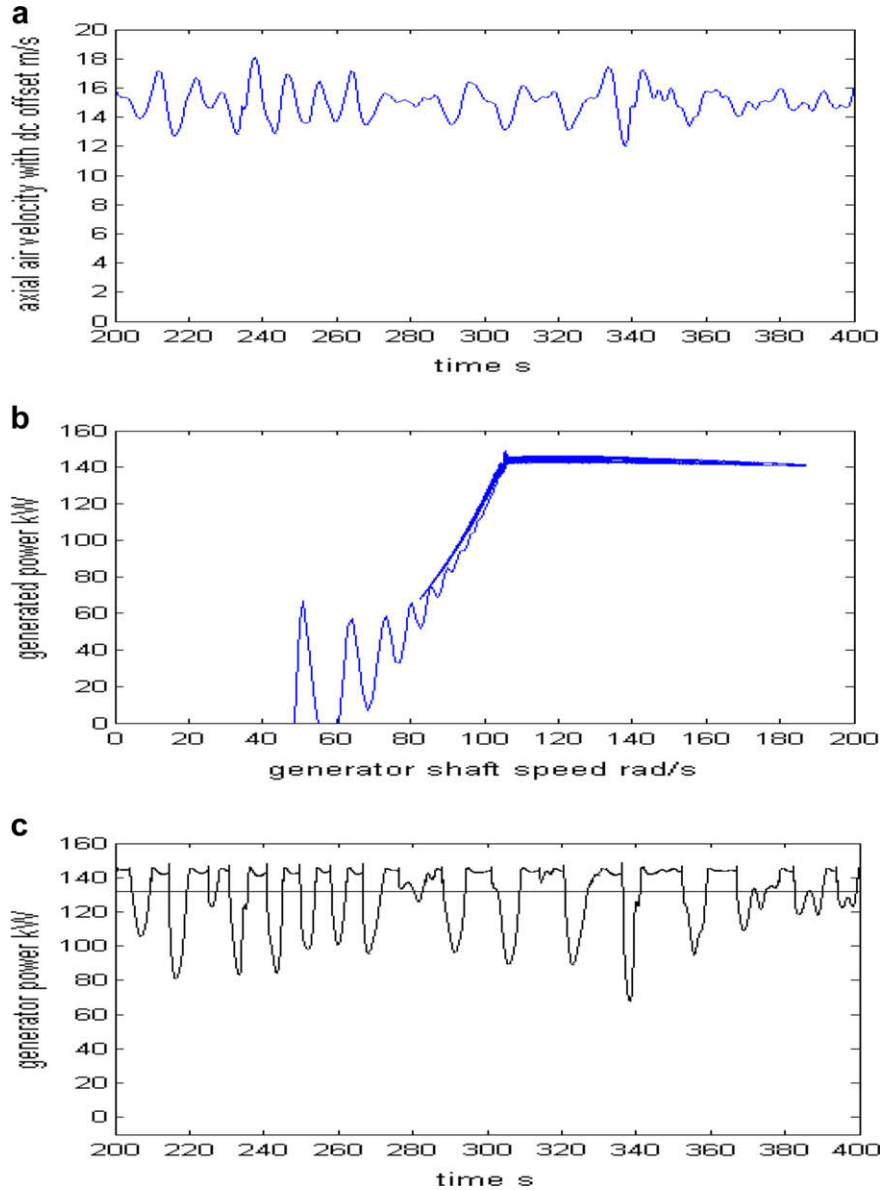


Fig. 9. (a) Fictitious wind speed data obtained by adding a DC offset. (b) Power trajectory for the fictitious wind speed. (c) Time variation of power for the fictitious wind speed.

until point R is reached, which is the peak power point. Here further acceleration cannot take place because the turbine power is less than the generator power on the right hand side. So equilibrium is attained at R, the peak power point.

Although the above discussion has been made as if the controller acts at discrete time intervals, it is not really so. The controller does not wait for point Q1 to be reached before changing the synchronous speed to ω_s . On the contrary, ω_s changes smoothly as the system accelerates, so that the difference $\omega - \omega_s$ is maintained constant throughout. Hence the turbine moves smoothly from P to R along the turbine curve for Vx_2 , whereas the generator will move smoothly along the cubical curve OR because the constant V/f^2 method with slip speed maintained constant at the proper value ensures that generator power moves along the cubical power curve corresponding to peak turbine power. Until point R is reached, turbine power is greater than generator power, ensuring that the system will accelerate. Exactly the reverse will happen if air velocity falls from Vx_2 to Vx_1 . The system will decelerate from R to O since turbine power goes below generator power. Thus the peak point is tracked without elaborate search strategies or complicated calculations.

3.1. Keeping the system within ratings

Although it is desired to maximize the generated power, it is also important to keep the limits of the system. The wind turbine has maximum speed limits and the generator and electronic converter have limits on the power they are capable of handling. Under these limitations it is not possible to operate the turbine at peak power and special conditions are required for the controller. These limits are included by dividing the control of the machine into regions as mentioned in Ref. [14].

The generated power is kept constant at the maximum permissible value by allowing the speed to increase. In this region the frequency of the converter is increased to prevent slip from increasing and to maintain generated power constant. Since the turbine power is in excess of the generated power, the system will accelerate. This can be allowed until the speed limit of the system is reached. After that, mechanical arrangements have to come into action to prevent air velocity from increasing further or blade pitch control has to be used to reduce C_p and turbine power output. This is shown in Fig. 6.

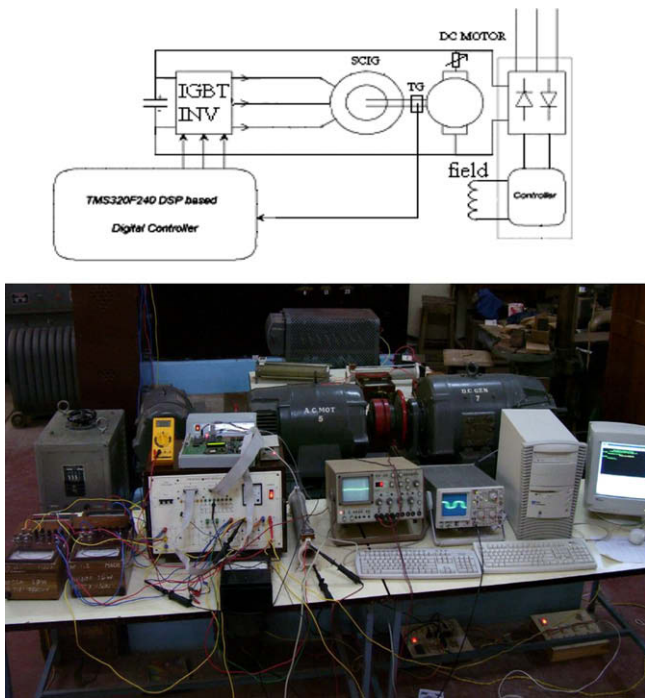


Fig. 10. Block diagram and photograph of the experimental setup.

There is a lower limit for the applied frequency and applied voltage. They cannot be made too low, since the machine needs a minimum excitation, and the turbine will stall at very low rotor speeds. Hence a lower limit is assigned to the frequency and the stator voltage. Since power levels are too low at these speeds, it is not worth tracking peak power anyway. Peak power cannot be extracted in these lower and higher limiting regions.

Unless the generator has been designed for the turbine or vice versa, there may be a mismatch. In particular, the rated turbine power may occur at a turbine shaft speed different from the generator shaft speed at which the generator rated power is reached. Hence, in order to match the two speeds, a suitable gearbox has to be selected.

4. Modeling and simulation

The proposed control logic is modeled and the real time performance of the system is investigated by simulating with measured air velocity data using MATLAB-SIMULINK [15,16]. The

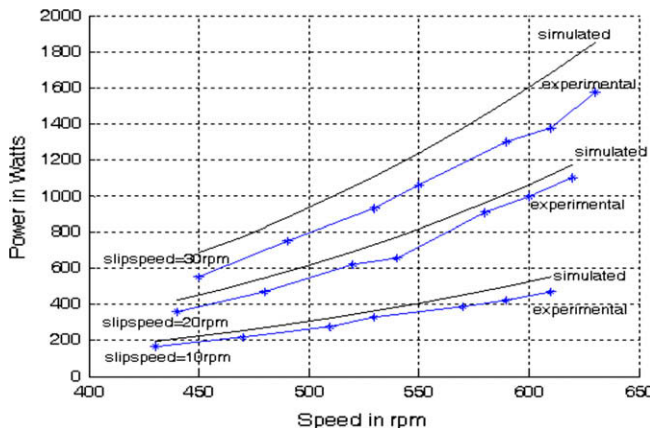


Fig. 11. Simulated and generated power for the laboratory induction generator at different slip speeds.

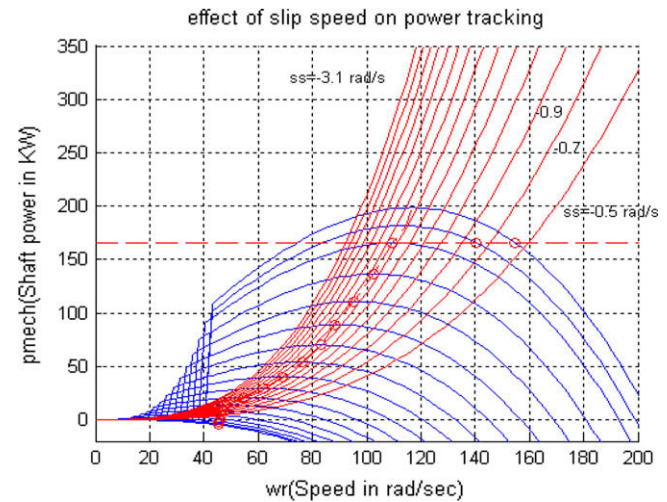


Fig. 12. Cubical power curves for slip speeds other than the correct one.

simulation diagram for the overall system is shown in Fig. 7. A gear ratio of 1.68 selected earlier has been included. It affects the effective values of turbine speed, turbine torque and turbine moment of inertia as seen by the generator, but does not affect the turbine power. The constant slip speed value of -1.7 rad/s to be maintained in the peak power tracking mode has been programmed. Once rated power is reached, the slip value is kept constant at -0.016 in order to maintain rated generated power.

5. Simulation results

The wave energy system was simulated with the air velocity data gathered from the Indian wave energy site [17]. The variation of generated power as a function of rotor speed obtained from the simulation is shown in Fig. 8b. The lower frequency limit is set to 20 Hz in order to start the turbine and also to avoid stalling of the turbine. When the rotor speed exceeds the corresponding synchronous speed (41.9 rad/s), generator operation starts and the controller enters the peak power tracking mode. The synchronous speed is maintained 1.7 rad/s below the rotor speed since this is the slip speed at which peak power is tracked for this particular turbine. The voltage is varied in proportion to square of frequency. Finally, when rated frequency and voltage are reached, constant power control starts. The voltage is maintained constant and frequency is increased such that slip is constant at -0.016 . This limits the power to approximately 160 kW , but allows the speed to increase above the rated speed. The machine must be designed to withstand up to 100% overspeed. Since wave energy is oscillatory, the system decelerates and accelerates in sympathy with the air velocity. The minimum speed is 41.9 rad/s whereas the air velocity peak determines the maximum speed. The hysteresis observed in the curve is owing to system inertia.

The average power is only 15.3 kW though peak power is 160 kW (Fig. 8c). This is typical of wave energy. The maximum speed attained is 170 rad/s . However, this result is encouraging compared to the uncontrolled system that produced only 7.86 kW for the same input [17]. Note the energy lost every 4 s in motoring due to recession of the waves. Thus the success of wave energy is greater in countries having predominantly high amplitude waves for a larger portion of the day. The air velocity in a wind energy system oscillates about a large positive value, rarely touching zero. Hence much higher powers can be expected. Adding a DC offset to the air velocity waveform as shown in Fig. 9a can prove this. The power trajectory for the fictitious wind speed is shown in Fig. 9b.

The time variation of power for the fictitious wind speed is shown in Fig. 9c.

The average power has now gone up to 132 kW.

6. Experimental setup

The block diagram and photograph of the experimental setup are shown in Fig. 10. A squirrel cage induction motor is used as an induction generator. The variable frequency variable voltage supply for the stator is obtained from an IGBT inverter. The PWM pulses for the inverter are obtained by programming a DSP kit based on the Texas Instruments TMS320F240 digital signal processor [18–20]. The IGBT inverter is supplied from a DC source obtained by rectifying three-phase AC supply using a diode full bridge rectifier. Since the diode rectifier cannot accept reverse power flow, the power is diverted back to the prime mover. The prime mover for the induction generator is a DC separately excited motor. It is used in place of the wind or wave turbine in the laboratory.

In order to emulate a wind/wave turbine, the DC motor is controlled through suitable power electronic converters and control circuits so that it has the same characteristic curve as the turbine at the site. The time variation of air velocity is sampled and recorded as a sequence of digital numbers in the memory of the DSP kit. At any instant the processor takes a sample of air velocity from the memory, takes a reading of the shaft speed from a digital tachometer, and calculates the torque that the prime mover must produce, by using a predefined turbine model. Then it gives proper pulses to the power electronic converters connected both in the armature as well as in the field circuits so that they apply proper voltages to the armature and field in order to produce the calculated torque at the shaft.

A digital tachometer was mounted on the shaft to measure the shaft speed at any instant and feed it to the DSP. The DSP was programmed to subtract a constant slip speed value from the actual speed to calculate the desired stator frequency. The stator voltage to be applied was next calculated by the DSP based on constant ratio of V/f^2 . Accordingly the binary numbers that control the frequency and modulation index of the PWM waveform were calculated in real time and the PWM signals were generated by the DSP. These signals were fed to the IGBTs in the inverter through opto-isolated drivers.

7. Experimental results

The DC motor (prime mover) was accelerated and decelerated by using both armature and field control in a manner so as to produce shaft speed variations similar to that observed at the wave energy site. The generated voltage, current and phase angle between the voltage and current were recorded using a digital power scope. The power was calculated and plotted against rotor speed. The experiment was conducted for three different values of slip speed, namely –10, –20 and –30 rpm. Simulated and experimental curves of generated power are shown in Fig. 11.

The experimental results show that for each slip speed there is a unique cubical curve. Depending on the turbine, one of these curves will pass through the peak power points. The other curves will not. Hence the correct slip speed to be maintained depends on the turbine characteristics. The effect of change in the slip speed setting on the power extraction in a wave turbine is shown for various slip speeds in Fig. 12.

The experimental results support the above conclusion.

8. Conclusion

When the peak power points for various air velocities are joined, they are found to lie practically on a cubic curve. Though

this fact has been known since early days, it has not been exploited for peak power tracking. It is shown that by varying the stator voltage in proportion to square of the stator frequency, the pull out torque is made to vary as square of speed and the corresponding power to vary as cube of speed. This ensures low slip operation throughout. Moreover, it is shown that only under this strategy does the slip speed corresponding to peak turbine power become constant at all speeds. This optimum value of slip speed can be obtained by conducting experiment at a single air velocity, which need not be measured. Then, by measuring the speed and applying a suitable stator frequency to the induction generator to maintain the desired slip speed, we can ensure that peak power is being tracked.

This strategy has advantages over V/f control. In the V/f control, slip frequency is variable with rotor speed, whereas in the present strategy it is constant. Also, the applied flux is unnecessarily high in the V/f scheme, producing higher no load losses. It is necessary to keep no load losses low since the generator operates at low power levels or even goes into motoring zone at low wind speeds. In case of wave energy, this happens every 4 s when air velocity passes through zero. In the proposed strategy, the flux level is reduced to the minimum needed to produce the desired torque (field weakening is inherent). Thus no-load losses are minimized, which means higher generated power for a given turbine shaft power. Thus, the new scalar control strategy does not require a wound rotor machine; hence it is cheap and easy to implement.

References

- [1] Buehring IK, Freris LL. Control policies for wind energy conversion systems. Pt C. IEE Proc Sept 1981;128(5).
- [2] Bhowmik Shibashis, Spee Rene, Enslin Johan HR. Performance optimization for doubly fed wind power generation systems. IEEE Trans Ind Appl July/Aug 1999;35(4):949–58.
- [3] Tan Kelvin, Islam Syed. Optimum control strategies in energy conversion of PMSC wind turbine system without mechanical sensors. IEEE Trans Energy Conversion June 2004;19(2):392–9.
- [4] Xu L, Cheng W. Torque and reactive power control of a doubly fed induction machine by position sensorless scheme. IEEE Trans Ind Appl May/June 1995;31(3):636–42.
- [5] Datta R, Ranganathan VT. A method of tracking the peak power points for a variable speed wind energy conversion system. IEEE Trans Energy Conversion Mar 1999;18(1):163–8.
- [6] Datta Rajib, Ranganathan VT. Direct power control of grid-connected wound rotor induction machine without rotor position sensors. IEEE Trans Power Electron May 2001;16(3):390–9.
- [7] Simoes MG, Base BK, Spiegel RJ. Fuzzy logic based intelligent control of a variable speed cage machine wind generation system. IEEE Trans Power Electron Jan 1997;12(1):87–95.
- [8] Li Hui, Shi KL, McLaren PG. Neural-network-based sensorless maximum wind energy capture with compensated power coefficient. IEEE Trans Ind Appl Nov/Dec 2005;41(6):1548–56.
- [9] Kazmierkowski M.P., D.L. Sobczuk, M.A. Dzieniakowski. Neural networks based current regulator for PWM inverters. In: Fifth European conference on power electronics and applications, 13–16 Sept 1993. Vol. 4, p. 186–9.
- [10] Bakhshai A., J. Espinoza, G. Joos, H. Jin. A combined artificial neural network and DSP approach to the implementation of space vector modulation techniques. In: IEEE Industry Application Society (IAS) annual meeting, San Diego, CA, 1996. p. 934–40.
- [11] Pinto JO, Bose BK, da Silva LEB, Kazmierkowski MP. A neural-network-based space-vector PWM controller for voltage-fed inverter induction motor drive. IEEE Trans Ind Appl Nov/Dec 2000;36(6):1628–95.
- [12] Zinger D.S., E. Muljadi, A. Miller. A simple control scheme for variable speed wind turbines. In: Proceedings of IEEE-IAS annual meeting; Oct 1996. p. 1613–8.
- [13] Nola F.J. United States patent 4,388,585; 1983.
- [14] Muller S, Deicke M, De Doncker RW. Doubly fed induction generator systems for wind turbines. IEEE Ind Appl Mag May/June 2002;8(3):26–33.
- [15] <<http://www.mathworks.com>>
- [16] MATLAB reference guide, 1997. USA: The Mathworks Inc.
- [17] Murthy B.K. Modelling and control of wave based wells turbine driven grid connected induction generator system, PhD thesis; 1998.
- [18] Texas Instruments. TMS 320F/C24x DSP controller-CPU and instruction set.
- [19] Texas Instruments. TMS 320F/C24x DSP controller-peripheral library and specific devices.
- [20] <<http://www.ti.com>>